1. Name and surname

Michał Paweł Ławniczak

2. Diplomas, academic/artistic degrees – please specify the title of the qualification, the place you graduated from as well as the year of obtaining the qualification and the title of the doctoral thesis.

PhD in Physics, Institute of Physics of the Polish Academy of Sciences, Warsaw 2011,
Thesis: *Study on Quantum Chaos in Open Systems*

MSc Eng, Faculty of Technical Physics, Information Technology and Applied Mathematics, Lodz University of Technology, Łódź 2006

3. Information on current employment with scientific/artistic establishments.

30.09.2010 to 29.09.2012	Employed as assistant at the Institute of Physics of the Polish Academy of Sciences
29.09.2012 to present	Employed as assistant professor at the Institute of Physics of the Polish Academy of Sciences

4. Scientific achievement forming the basis for habilitation procedure.

In accordance with Article 16 Section 2 of the Act of 14 March 2003 on the Academic degrees and academic titles and on artistic degrees and title, I hereby present as the achievement, the series of publications entitled:

Analysis of spectral and scattering properties of systems in which the phenomenon of wave chaos occurs

H1. **M. Ławniczak**, L. Sirko, *Investigation of the diagonal elements of the Wigner's reaction matrix for networks with violated time reversal invariance*, Scientific Reports **9**, 5630 (2019)

H2. **M. Ławniczak**, M. Białous, V. Yunko, S. Bauch, L. Sirko, *Missing-level statistics and analysis of the power spectrum of level fluctuations of three-dimensional chaotic microwave cavities*, Phys. Rev. E **98**, 012206 (2018)

H3. O. Hul, **M. Ławniczak**, S. Bauch, A. Sawicki, M. Kuś, L. Sirko, *Are Scattering Properties of Graphs Uniquely Connected to Their Shapes?*, Phys. Rev. Lett. **109**, 040402 (2012)


NEWSPAPER

PHYSICAL REVIEW LETTERS

Contents

Articles published 21 July–27 July 2012

VOLUME 109, NUMBER 4 27 July 2012

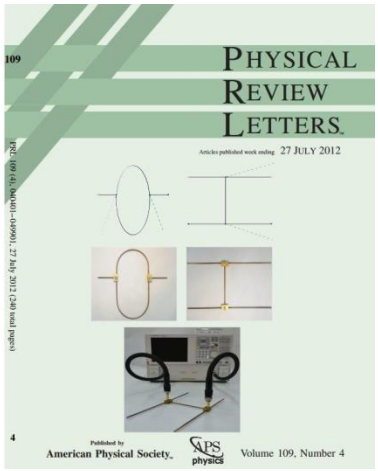
109

PHYSICAL REVIEW LETTERS

Articles published week ending 27 JULY 2012

Published by American Physical Society

Volume 109, Number 4

H4**. M. Ławniczak**, A. Sawicki, S. Bauch, M. Kuś, L. Sirko, *Resonances and poles in isoscattering microwave networks and graphs,* Phys. Rev. E **89**, 032911 (2014)

H5. **M. Ławniczak**, J. Lipovský, L. Sirko, *Non-Weyl microwave graphs,* Phys. Rev. Lett. **122**, 140503 (2019)

Introduction

The notion of deterministic chaos was introduced to science as early as the 19th century by a French mathematician Henri Poincaré **(1)**. In 1963 the notion was popularised by a meteorologist called N.E. Lorenz, who, as a result of the work on a system of three nonlinear differential equations modelling the phenomenon of thermal convection in the atmosphere, discovered that for a specified set of system parameters, the system is chaotic **(2).** The Lyapunov exponent is a measure of the chaotic nature of classical systems

Unfortunately, in the case of quantum systems, the criterion related to the exponential rate of separation of trajectories in the phase space (positive Lyapunov exponent) becomes useless. This results from the Heisenberg uncertainty principle. According to the principle, simultaneous measurement of position and momentum observables is possible only with finite precision. Therefore, in the phase space it is not possible to study the orbits of the system with arbitrary precision. That is why we are looking for new ways to describe and study quantum chaotic systems.

Recently, the interest in studies of the chaotic quantum systems has significantly grown. Due to the extreme difficulties encountered in experiments, mainly theoretical studies of quantum

chaotic systems are conducted. For this reason, experimental verifications are very valuable and desired.

Standard methods of verifying of system chaoticity, rely on testing statistical properties of its energy spectrum in its discrete range. In case of using spectrum correlation functions such as nearest neighbour spacing distribution (NNSD) or spectrum stiffness (Δ_3), it is very important to know all the eigenvalues of energy in the analysed range **(3)**. Consequently, the knowledge of the complete spectrum of the studied system is particularly important. Unfortunately, loss of energy states is practically unavoidable, particularly in case of experimental research. It happens because of the possible degenerations or overlapping of states due to their finite width resulting from the internal absorption as well as from the openness of the system. In case such as this, it is necessary to use more advanced methods for analysing the experimental results which take into account such factors as dependence of short-range and long-range correlation functions on the number of lost states.

Methodology of research

The research focused on microwave networks and cavities, which, in the case of one and two-dimensional systems, simulate quantum graphs and quantum billiards, as well as on three-dimensional microwave cavities in which the phenomenon of wave chaos occurs.

Graphs are single-dimension quantum systems connected in vertices, creating a network structure (fig. 1). For the first time, the concept of quantum graphs was used by L. Pauling in the research on free electrons in molecular chains **(4).** Graphs are also used in the research of other systems and phenomena, such as superconducting quantum systems **(5)**, quantum gravity model with discrete evolution in time **(6)** and even Alzheimer's disease **(7)**.

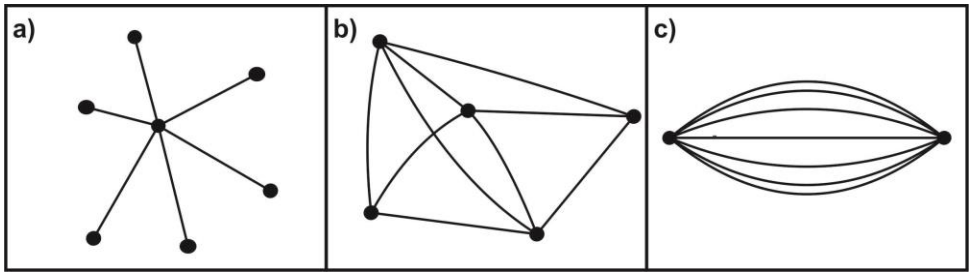

Fig. 1
Examples of different topologies of quantum graphs.

In the experimental research, the quantum graphs are simulated by microwave networks **(8; 9; 10)** (fig. 2a). A network is made up of microwave cables – appropriately connected in their vertices

(fig. 2b). The cables act as graph arms and the microwave joints, produced at our laboratory, constitute the graph vertices.

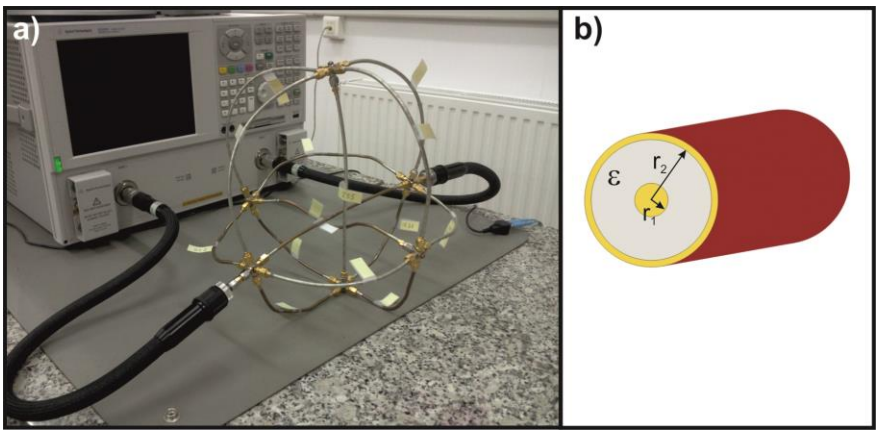

Fig. 2

a) Photograph of a microwave network simulating a six-vertex, fully connected graph.
b) Microwave cable cross-section diagram. The cable is made up of two cylindrical conductors with the radii r_1 and r_2 and a dielectric material filling in the space between them, having dielectric constant ε.

This simulation is possible up to the frequency of $v_c = \frac{c}{\pi(r_1+r_2)\sqrt{\varepsilon}}$, below which only the wave in the basic TEM mode propagates in the cable. Then, the telegraph equations for the network arms

$$\frac{d^2}{dx^2}U_{ij}(x) + \frac{\omega^2\varepsilon}{c^2}U_{ij}(x) = 0 \tag{1}$$

are analogous to the Schrödinger equations for the graph arms

$$\frac{d^2}{dx^2}\Psi_{ij}(x) + E\Psi_{ij}(x) = 0. \tag{2}$$

In the above equations, the wave function $\Psi_{ij}(x)$ describes the motion of particle in the graph arm connecting vertices i with j and fulfils there the Dirichlet $\left(\Psi_{ij}(x) = 0\right)$, or the Neumann boundary conditions (function continuity). The $U_{ij}(x)$ means the potential difference between the cable coaxial conductors.

The equations are analogous assuming that $\frac{\hbar}{2m} = 1$, where m is the mass of the particle moving in the graph arms, $\Psi_{ij}(x) \Leftrightarrow U_{ij}(x)$, and the role of energy E is fulfilled by the square of wave vector $k^2 = \frac{\omega^2\varepsilon}{c^2}$.

In order to simulate quantum graphs with a broken time reversal symmetry relative to time, i.e. systems which the statistical properties of the energy eigenvalues are the same as eigenvalues of unitary matrices (Gaussian Unitary Ensemble – GUE, $\beta = 2$) described in the random matrix theory (RMT), microwave circulators were placed in the network vertices (fig. 3a).

Figure 3b shows the circulator operating principle. The wave entering the first port of the device can exit it only via the second port, the wave entering the second port can exit only via the third port and the wave entering the third port can exit the circulator only via the first port.

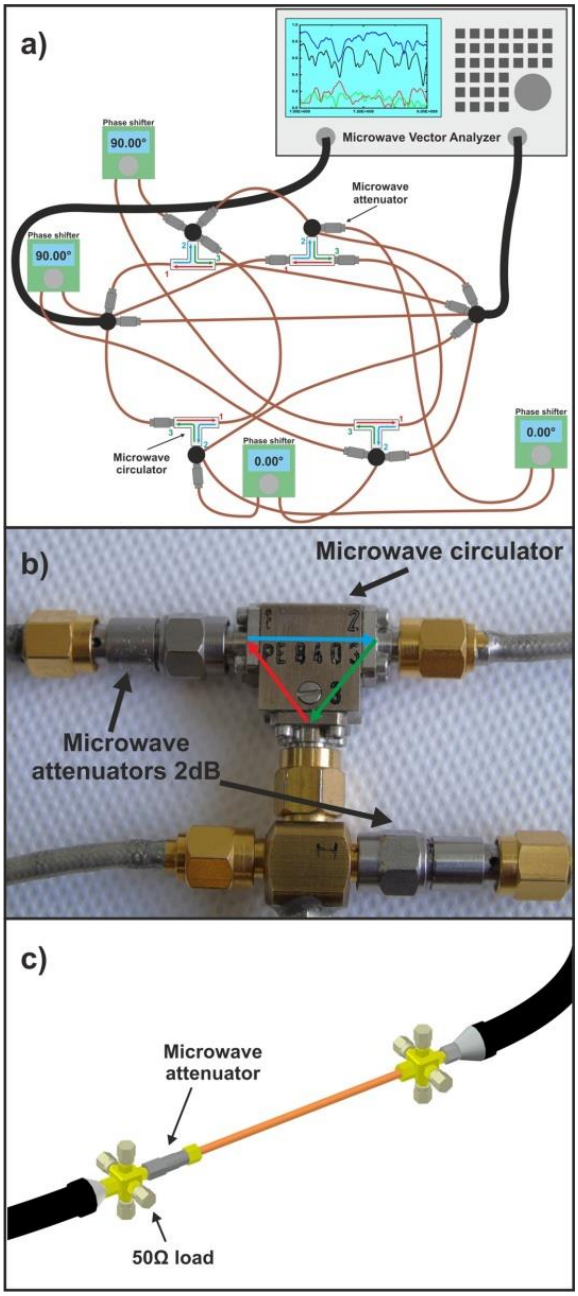

Fig. 3

a) Diagram of the measuring system used for simulation of graphs with a broken time reversal symmetry. Microwave circulators and attenuators are introduced to the network.
b) Photograph of a microwave circulator with directions of signal propagation marked. The photograph also shows 2 dB attenuators.
c) Diagram of the experimental setup used for the elimination of direct processes.
The figure was published in **H1**

A network without circulators simulates a graph with a time reversal symmetry (Gaussian Orthogonal Ensemble – GOE, $\beta = 1$) in the RMT. It should be emphasised that there are papers

showing the possibility of using microwave networks with circulators to study the systems with a spin (Gaussian Symplectic Ensemble – GSE, $\beta = 4$ **(11)**).

Therefore, microwave networks are unique objects that make it possible to experimentally study the three symmetry classes defined in the RMT.

Other interesting and important systems in research of quantum chaos, microwave cavities simulating two-dimensional (2D) quantum billiards (12; 13; 14; 15; 16) were considered in my publications listed with a brief description in item 5 of this manuscript.

With the help of the Vector Network Analyzer (VNA), we measured the spectrum of the scattering matrix, both of microwave networks and cavities. The Agilent E8364B analyser (fig. 2a) enabled single and double-port measurements. The result of single-port measurement is a one-element scattering matrix $S = \sqrt{R}e^{i\Theta}$ and of the double-port measurement, a four-element matrix:

$$\hat{S} = \begin{bmatrix} S_{11} & S_{12} \\ S_{21} & S_{22} \end{bmatrix}. \quad (3)$$

Diagonal elements of the matrix are related to signals entering the system and exiting it via the same input/output (reflected from the system.) The non-diagonal elements are related to the signals passing through the system from one port to the other (fig. 5).

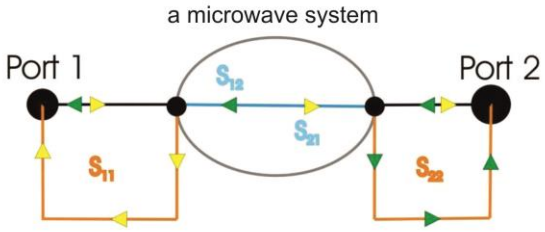

Fig. 4
Presentation of signals and the corresponding scattering matrix elements $\hat{S}$ for double-port measurement.

Analysis of the problem of lost eigenvalues in the spectra of the systems simulating chaotic quantum graphs.

At the beginning, it was mentioned that much research on chaotic quantum systems consists in the analysis of statistical properties of the energy spectra of such systems. Therefore, in such research, the possibility of finding as many energy levels as possible is so important. This is a serious problem, particularly in case of analysing experimental spectra of real physical systems, as for example in the case of research on atomic nuclei or particles **(20; 21; 22; 23)**.

One of the reasons for losing the states is the overlapping of energy levels resulting from their finite width connected with the absorption in the real physical systems. In the work **H1** the author describes his research of a system with strong absorption. As part of this research, he constructed a six-vertex fully connected network, i.e. each of the six vertices was connected with each of the other ones.

Microwave circulators were introduced to four network vertices (fig. 3a). Thus, the network simulated a hexagonal quantum graph with broken time symmetry, i.e. a GUE-type system in the RMT. Strong absorption in the system was achieved by introducing 1 dB and 2dB microwave attenuators to the network arms. Figure 3b shows the 2dB attenuators. Figure 3c shows the measuring system, which was used to eliminate the so-called 'direct processes.' These processes result from the reflection of part of the signal before entering the system and from the signal passing directly through the cable connecting the entry/exit vertices. For the networks which were constructed, the author measured the spectra of their scattering matrix $\hat{S}$, for each realisation of the network implementations, distinguished by their arm lengths. The arm lengths were modified with the help of phase shifters (fig. 3a).

The introduction of strong absorption lead to the impossibility of correctly determining the resonance positions in the obtained spectra. The measure of effective absorption is the coefficient: $\gamma = \frac{2\pi\Gamma}{\Delta} = \gamma_{abs} + T_a + T_b$. In this expression, Γ is the average resonance width, Δ the average distance between them. $T_{i=a,b}$ means the transmission which is the measure of openness of the system, i.e. of the connection of the system with the surroundings and γ_{abs} is an internal absorption strength. In case of author's experiments, the network was connected to the surroundings via the cables introducing signals to and from the a and b ports of the microwave analyzer. In a theoretical analysis, a cable can be considered as an arm of infinite length, connecting the graph with the external world.

For the network with 1 dB attenuators, the mean coefficient $\langle\gamma\rangle$ was equal to 19.4. After applying 2 dB attenuators, the mean value of $\langle\gamma\rangle$ increased to 48.4. The author obtained the values by fitting the experimental distributions of the reflection coefficient $P(R)$ with the theoretical distributions **(24)**. The obtained distributions and the fitted theoretical curves are shown in figure 5. Red, empty circles show the experimental distributions for the network with 1 dB attenuators and the red, full circles show the distribution for the network with 2dB attenuators. Next, the author compared the experimental distributions of the real and imaginary parts of Wigner's reaction matrix $\widehat{K}$ with the theoretical distribution predicted for the obtained values of γ. Wigner's reaction matrix is linked with the scattering matrix by the following relation:

$$\widehat{K} = i\frac{\hat{S} - \hat{I}}{\hat{S} + \hat{I}}. \tag{4}$$

The real part of Wigner's matrix is shown in figure 6, the imaginary part in figure 7. The distribution is presented with the same symbols as in figure 5.

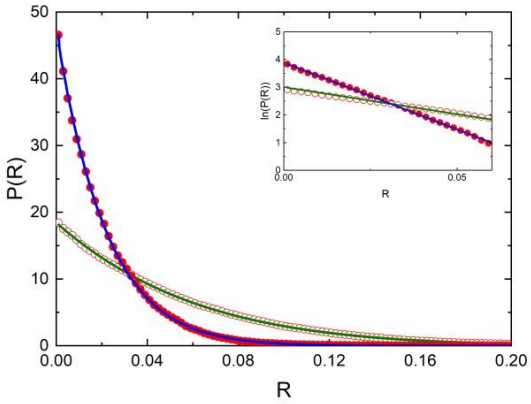

Fig. 5

Experimental distributions of the reflection coefficients obtained for microwave networks with 1 dB attenuators (red, empty circles) and with 2 dB attenuators (red, full circles). The experimental distributions were compared with the theoretical predictions (corresponding solid lines)
The figure was published in H1.

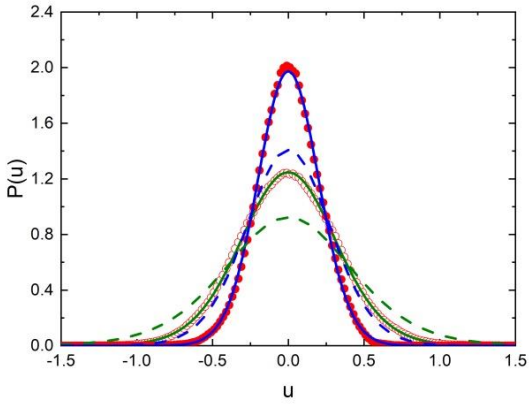

Fig. 6

Experimental distributions of the real part of the Wigner's reaction matrix obtained for microwave networks with 1 dB attenuators (red, empty circles) and with 2 dB attenuators (red, full circles). The experimental distributions were compared with the theoretical predictions (corresponding solid lines)
The figure was published in H1.

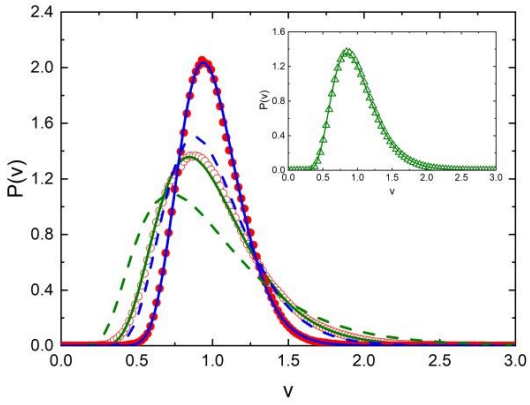

Fig. 7

Experimental distributions of the imaginary part of the Wigner's reaction matrix obtained for microwave networks with 1 dB attenuators (red, empty circles) and with 2 dB attenuators (red, full circles). The experimental distributions were compared with the theoretical predictions (corresponding solid lines)
The figure was published in H1.

The results are in very good agreement with the theoretical predictions shown with the solid lines. In addition, in **H1**, the author has shown that in the presence of strong internal absorption, the impact of channel openness is negligible and the studied distributions can be approximated by exponential expressions **(25)** (insert in fig. 6 and fig. 8).

The obtained results show that the distributions $P(v)$ and $P(u)$ of the imaginary and the real parts of the diagonal elements of the Wigner's reaction matrix $\widehat{K}$ together with the elastic

enhancement factor W_β can be used to determine the absorption of the system and to unique identification of the system's class of the time symmetry.

The elastic enhancement factor W_β is another measure, apart the Wigner's reaction matrix, which can be used for the purposes of verifying the chaotic character of the system, when the complete spectrum of energy levels cannot be determined. The enhancement factor has been used in the nuclear physics research **(26; 27; 28)** and is defined as a ratio of the variance of diagonal elements of a two-port matrix $\hat{S}$ to the variance of its non-diagonal elements **(29)**. The value has been already studied in chaotic systems **(30; 31; 32)**.

In the work **H2** the author has shown how to obtain the information about the number of the missing eigenvalues of energy in the experimentally obtained spectrum of a chaotic system. This knowledge is particularly valuable in the analysis of experimental results, when due to the degeneration and / or overlap of resonances of the studied system, it is impossible to detect all of them.The paper **H2** presents how we can do it on the example of the matrix spectra obtained in two-port measurements S, for three-dimensional chaotic microwave cavity. Rough walls and the slightly convex bottom of the cavity were decisive for the chaotic nature of the system (fig. 8). Various configurations of the system were achieved by rotating the scatterer (fig. 8a) placed inside and by changing the position of the antennas (positions A_1, A_2, A_3 figure 8a).

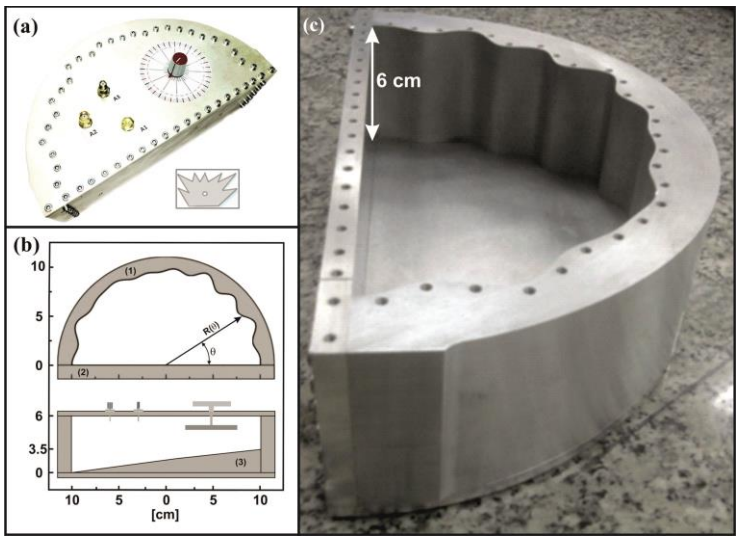

Fig. 8

Three-dimensional microwave resonance cavity.
a) Picture of a closed cavity, showing the position of antennas A_1, A_2, A_3. The insert shows the shape of the scatterer placed inside the cavity.
b) Diagram of the cross section and the vertical section of the cavity. Elements (1) and (2) were decisive for the chaotic character of the system.
c) Picture of the interior of the cavity
The figure was published in H2.

In the case of such a system there is no formal analogy between the Schrödinger equation for a three-dimensional quantum billiard and the three-dimensional Helmholtz equation. This is due

to the fact that the electromagnetic field cannot be described with a scalar function such as the wave function. Despite that, it was shown that some dependencies assumed for chaotic quantum systems, e.g. nearest neighbour spacing distribution (NNSD), are the same as the dependencies obtained for three-dimensional chaotic resonance cavities **(33; 34)**. This encouraged the author to also study 3D systems.

In order to determine the number of lost states, short and long-range correlation functions of the energy levels are used. First, short-range correlations are calculated. In the work in question, this was the nearest neighbor distribution. Figure 9a presents the NNSD (histogram) experimental distribution published in **H2**, together with the theoretical predictions for two cases: complete spectrum (black, solid line) and incomplete spectrum, with the lack of 11% of eigenenergies (red, dotted line) **(35)**. Figure 9b shows the integrated NNSD. The number of the lost eigenstates is determined by the parameter φ, the fraction of observed levels, with a value from the range $\langle 0; 1 \rangle$, where 1 means a complete spectrum and 0 all states are missing. According to the figure, the nearest neighbour spacing distribution is not very sensitive to the number of lost states (Fig. 9a,9b).

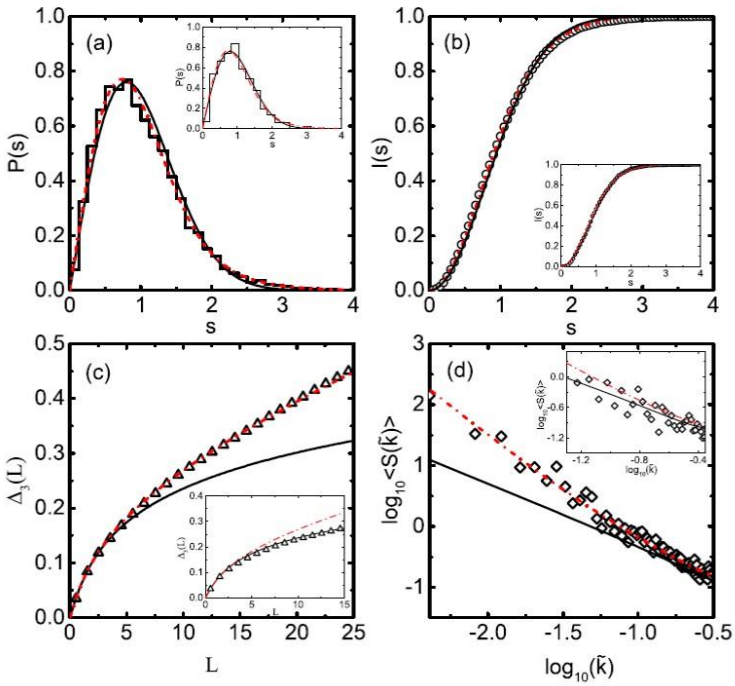

Fig. 9

Experimental distributions of correlation functions obtained for a three-dimensional microwave cavity. The distributions were obtained for $\boldsymbol{\varphi = 0.89}$. The results were compared with the theoretical predictions for the case of a complete spectrum (black, solid lines) and for the case of loss of 11% of eigenenergies (red, dotted lines). The inserts in figures b, c and d show the experimental distributions obtained from complete spectra of nine configurations in the frequency range of 7-9 GHz.

a) Nearest neighbour spacing distribution (black bars).
b) Integrated NNSD (black rings).
c) Distribution of function $\Delta_3(L)$ (black triangles).
d) Distribution of function $S(\tilde{k})$ (black, empty diamonds).
The figure was published in H2.

However, determination of NNSD gives a clear answer to the question whether the system is chaotic and to which class of the symmetry at RMT it belongs. With this knowledge, it is possible to calculate the corresponding long-range correlation functions such as Σ^2 and Δ_3. The work **(35)** shows the dependence of the said functions from the parameter φ. The number of the lost energy states can therefore be obtained by fitting the value φ so that the theoretical distribution matches the experimental distribution as closely as possible. Such fitting, for the function Δ_3 is shown in figure 9c, where the black and red solid lines are the theoretical curves for $\varphi = 1$ and $\varphi = 0.89$ and the triangles indicate the experimental data. As we can see, these functions are much more sensitive than NNSD to the number of lost eigenvalues.

Another correlation function, even more sensitive to the number of missing energy levels, is the power spectrum of discrete and finite series $S(\tilde{k})$. Comparison of the experimental distribution (diamonds) with the fitted theoretical curve (red, dotted line) shown in figure 9d confirms that 11% of resonances are lost in the experiment.

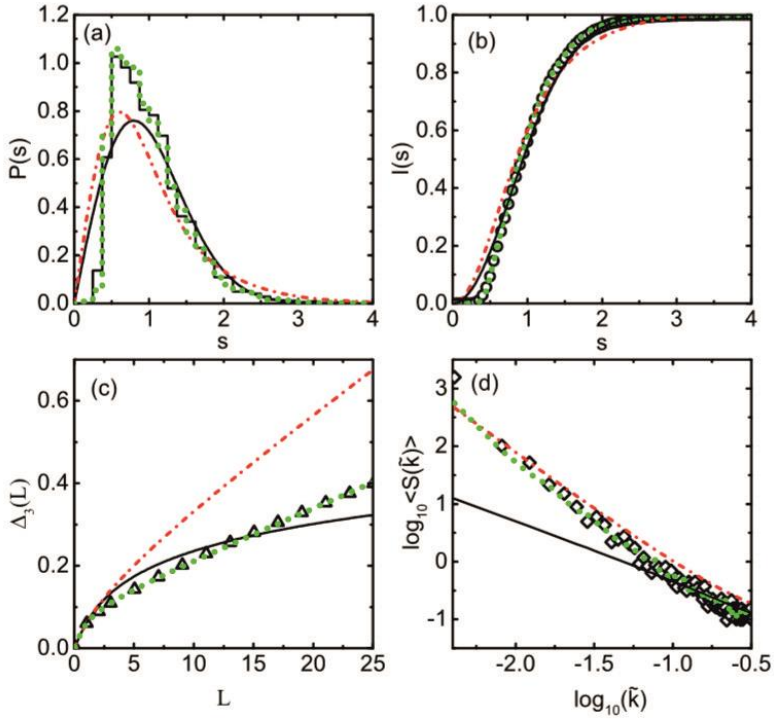

Fig. 10

Distributions of the correlation function obtained for a three-dimensional microwave cavity. The distributions were obtained for modified experimental data $\varphi = 0.7$. Resonances were lost in a non-random way. The results were compared with the theoretical predictions (red, dotted lines) and with the ones obtained using the eigenvalues of random matrices (green, dotted lines).

a) Nearest neighbour spacing distribution (black bars).

b) Integrated NNSD (black circles).

c) Distribution of function $\Delta_3(L)$ (black circles).

d) Distribution of function $S(\tilde{k})$ (black, empty squares).

The figure was published in H2.

It should be underlined that the procedure is successful even for $\varphi = 0.5$. This was verified by randomly decreasing the number of experimentally identified resonances by 39 p. p (percentage points) and fitting the such reduced set of experimental data with the corresponding theoretical curves.

Additionally, in **H2** the author analysed the usability of the method for the case when the states are lost mostly due to the overlapping of resonances. For that purpose, the two closest resonances of the experimental spectrum ($\varphi = 0.89$) were found and one of them was removed. The procedure was repeated until achieving $\varphi = 0.7$. It turned out that consistence with theoretical predictions was not achieved for such a case, both for short and long-range correlation functions (red, dotted lines – theory, modified experimental data – histogram, circles, triangles and squares in the figure 10). The obtained results show that the presented method is not successful when the lost energy states are correlated. In order to confirm this observation, eigenvalues of random matrices were generated and then 30% of them were removed in the same way as they were lost in the experimental spectra. At first, 11% of them were randomly removed. Then one of the two closest eigenvalues also was removed until achieving $\varphi = 0.7$. For the so-modified strings of eigenvalues of random matrices, correlation functions were calculated (green, dotted, lines in figure 10). The obtained distributions of the functions are consistent with those obtained for the modified experimental spectra.

The above investigations made a constructive contribution to Vitalii Yunko's doctoral thesis of which I was a supporting promoter. In the chapter VIII, dr Yunko showed the results obtained for the smaller fractions of observed resonances than in the work of **H2** ($\varphi = 0.85$ and $\varphi = 0.65$, respectively), testing the limit of the method.

Properties of quantum graphs resulting from their topology

When studying the systems where eigenvalues were lost in the experimental spectra, the author became interested in the issue of the properties of quantum graph and microwave network spectra resulting from their topology.

As it turned out, by constructing quantum graphs with appropriate topology, isoscattering systems (systems that scatter in the same way) or systems with the number of energy eigenvalues lower than the value according to the Weyl's law can be obtained.

Isoscattering quantum graphs

The first problem related to the topology of quantum graphs researched by the author was verifying whether two systems can exist which scatter electromagnetic waves in the same way, despite different shapes. The research resulted in the publications **H3, H4.**

The work **H3** is entitled *Are Scattering Properties of Graphs Uniquely Connected to Their Shapes?* The prestigious journal Physica Review Letters distinguished this publication, putting the photograph of the experimental system described in the paper on the issue cover. The title refers to the famous question asked by Mark Kac in 1966: *''Can one hear the shape of a drum?''* **(36)**. The question proved to be so nontrivial that the answer to it was given only almost thirty years later. In 1992 C. Gordon, S. Webb and S. Wolpert, applying the T. Sunada theory **(37)** presented two two-dimensional systems having different shapes but the same spectrum of eigenenergies **(38; 39)**. This theoretical reasoning was confirmed in experiments two years later by S. Sridhar and A. Kudroli **(40)**.

The research in the area of quantum graphs related to Mark Kac's question was started by B. Gutkin and U. Smilansky **(41)**. The subject was continued in a series of papers **(42; 43; 44; 45)**

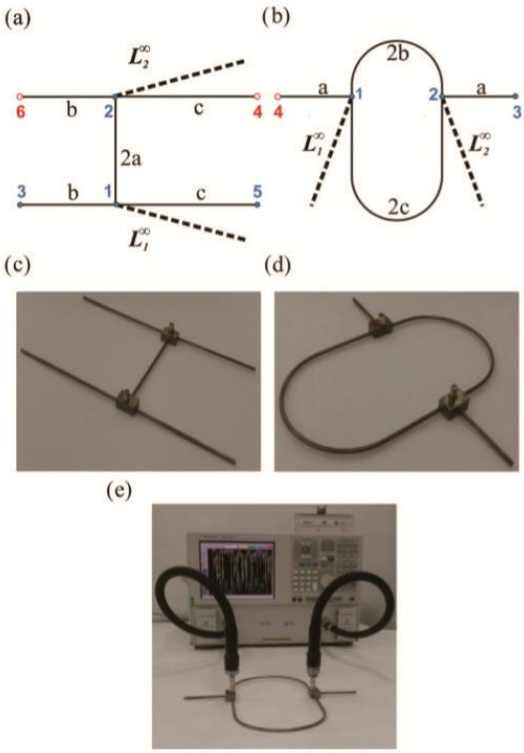

Fig. 11

The experimental setup for measuring the spectrum of four-element scattering matrix $\hat{S}$ of two microwave networks of different shapes and the same spectrum of determinant of matrix $\hat{S}$.
a) and c) Diagram and photograph of six-vertex network, respectively (network I)
b) and d) Diagram and photograph of four-vertex network, respectively (network II).
e) Photograph of the four-vertex network connected to the Vector Network Analyzer.
The figure was published in H3.

In the papers **(44; 45)**, the authors developed the Sunady theory, presenting the method of obtaining a pair of quantum graphs with different topologies but the same spectrum. Channels connecting the graphs with the external world are their important elements.

The author is the first who experimentally verified this method. For that purpose, appropriate microwave networks were prepared. One network was a six-vertex network with five arms (network I). The other network had four vertices and four arms (network II). The networks differed also in terms of boundary conditions at the vertices. The first one had two vertices with Dirichlet boundary conditions and the other had only one such vertex. The graph diagrams and the photographs of the networks prepared in our laboratory were included in the paper **H3** and are shown in figure 11a, b and 11c, d. above.

For both systems, two-port spectral measurements of the four-element scattering matrix $\hat{S}$ were made (fig. 11e).

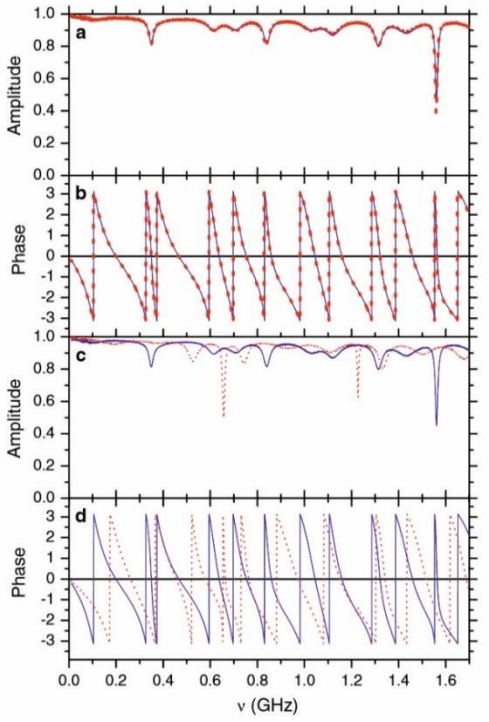

Fig. 12

Experimental spectra of the determinant of four-element scattering matrix $\hat{S}$.
a) Amplitude of determinant of matrix $\hat{S}$ obtained for the six-vertex network (network I, red circles) and the four-vertex network (network II, blue solid line).
b) Phase of determinant of matrix $\hat{S}$ obtained for the six-vertex network (network I, red circles) and the four-vertex network (network II, blue solid line).
c) Amplitude of determinant of matrix $\hat{S}$ obtained for the six-vertex network (network I, red circles), in which Neumann boundary conditions were changed into Dirichlet boundary conditions at one of the vertices and the four-vertex network (network II, blue solid line).
d) Phase of determinant of matrix $\hat{S}$ obtained for the six-vertex network (network I, red circles), in which Neumann boundary conditions were changed into Dirichlet boundary conditions at one of the vertices and the four-vertex network (network II, blue solid line)
The figure was published in H3.

Next, the author calculated the determinants of both spectra. Within the frequency range 0.01-1.7 GHz, both the amplitudes $\left|det\left(\hat{S}(v)\right)^{(\mathrm{I})}\right| = \left|det\left(\hat{S}(v)\right)^{(\mathrm{II})}\right|$ (fig. 12a) and the phases of the determinants $Im\left[log\left(det\left(\hat{S}(v)\right)^{(\mathrm{I})}\right)\right] = Im\left[log\left(det\left(\hat{S}(v)\right)^{(\mathrm{II})}\right)\right]$ (fig. 12b) are identical. The red points in figure 12 mark the spectra of the determinant of the scattering matrix for the six-vertex network (I) and the blue solid line marks the spectra for the four-vertex network (II).

In addition, the spectrum of the first network (I) was measured after changing the boundary condition at one its vertices. The Neumann boundary condition was replaced by a Dirichlet boundary condition. Following that, the networks cease scattering in the same way (fig. 12c and 12d).

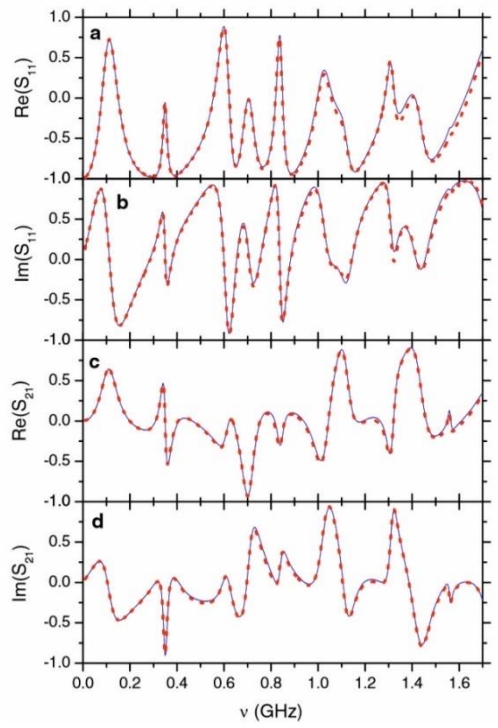

Fig. 13

Experimental spectra of the scattering matrix elements $\hat{S}$ for the six-vertex network (network I, red circles), and spectra obtained from the spectrum of the four-vertex network (network II) using the transformation matrix T (blue solid line). The figure was published in H4.

An important result of the **H3** work is the experimental verification of the transplantation relationship:

$$\hat{S}(v)^{(\mathrm{II})} = T^{-1}\hat{S}(v)^{(\mathrm{I})}T, \qquad (5)$$

where $T = \begin{bmatrix} 1 & -1 \\ 1 & 1 \end{bmatrix}$. Thanks to this relationship if the elements of the matrix $\hat{S}$ of one network are known, it is possible to calculate the elements of the scattering matrix for the second network. In figure 13 the author presents the spectra of the scattering matrix elements $\hat{S}$ obtained as a result of

transformation of the four-vertex network scattering matrix (II) (blue solid line). The red points mark the spectra of elements $\widehat{\boldsymbol{S}}$ of the six-vertex network (I). As we can see, the spectra are indistinguishable with very high accuracy .

In the paper **H4** the author has shown the results for isoscattering networks within a broader frequency range 0-3 GHz. A higher frequency, i.e. smaller wave length, leads to a significant increase of sensitivity to any imperfections of the measurement system. Elimination of such imperfections poses a huge challenge for the experimental researchers.

In the paper **H4** the author considers the significant local features characterising both graphs, such as poles of matrix $\hat{S}$ and structures of the resonances. It was demonstrated that the presented graphs are isopolar. This means that they have the poles of the determinant of the scattering matrix in the same points of the complex frequency plane. We should note that isopolar graphs do not need to be isophasic ones, i.e. graphs which have the same phase spectrum. However, when a graph is isophasic, it is also isopolar. In the paper **H4**, the coordinates of the position of the pole of matrix $\hat{S}$ on the complex plane were determined. The positions are related to the eigenvalues of the wave vector, which are the solutions of the telegraph equation. Eigenvalues of the wave vector, as the equivalent of eigenenergies of quantum graphs can be written as $k_l = \frac{2\pi}{c}(v_l + i\Delta v_l)$ where Δv_l is the half-width of the resonance and the coordinates of a scattering matrix pole are: $(v_l, \Delta v_l)$.

The author compared full widths of resonances of the experimental spectrum Δv^{exp} with the calculated pole positions $\left(v^{cal}, \Delta v^{cal}\right)$ and obtained $\langle\frac{\Delta v^{exp}}{2\Delta v^{cal}}\rangle = 0.99 \pm 0.13$, which confirms the high quality of the experiments performed. In **H4**, there is also an analytical formula for calculating all four elements of the scattering matrix $\hat{S}$ derived by Adam Sawicki.

Weyl and non-Weyl quantum graphs

Another subject of the author's research connected to the graph topology was related to the possibility of obtaining the non-Weyl graphs **H5**. According to Weyl's law, density of graph eigenvalues $\rho = \frac{\pi}{\mathcal{L}}$ when their number tends to infinity. $\mathcal{L} = \sum_i \ell_i$ is the sum of graph arm's length. Therefore, the density remains unchanged as the function of frequency and depends only on the total length of the graph $\mathcal{L}$. For closed graphs (graphs that do not have channels connecting them to the external world) the number of eigenvalues in the range of $(0, R)$ is given by the expression **(46):**

$$N(R) = \frac{\mathcal{L}}{\pi}R + O(1), \tag{6}$$

where $O(1)$ is the function, which tends to 1 for $R \to +\infty$.

In the case of microwave networks, the number of resonances in the frequency range $(0, v)$ can be written as:

$$N(v) = \frac{\mathcal{L}}{\pi} v + O(1). \tag{7}$$

Connecting the channels makes the graph an open system. One could expect that such change does not affect the number of energy levels but only their width. However, according to E. B. Davis and A. Pushnitski **(47)**, this is not always true. It was proven that there are graphs, for which the number of energy levels is smaller than the number predicted with the formula 7. Such graphs are referred to as non-Weyl graphs in contrast to the graphs for which the equation 7 is satisfied, referred to as Weyl graphs. In the paper **(47)** demonstrated that there is a simple topological condition for making possible such a distinction. A graph becomes a non-Weyl graph only when there is a vertex, on which the number of graph arms and the number of channels opening the system is the same (vertex 1 in fig. 14b). This vertex is called a balanced vertex. In the papers **(48; 49)** it was verified that this condition determines the creation of a non-Weyl graph also for various boundary conditions at other vertices and in the presence of magnetic field**.**

In the paper **H5** the author presents the experimental results for the pair of microwave networks designed and prepared by him. The only difference between them was the points of channel connections. Vector analyzer cables acted as channels (fig. 14c and d). As it is shown in figure 14, one of the networks has a vertex connecting two internal arms and two analyzer cables (vertex 1 in panels b and d) - balanced vertex.

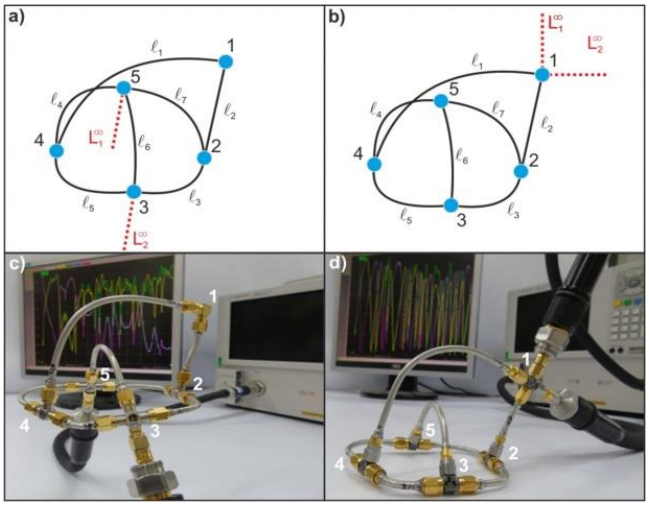

Fig. 14

a) and c) diagram and photograph of the network simulating a Weyl graph, respectively.
b) and d) diagram and photograph of the network simulating a non-Weyl graph, respectively.
The figure was published in H5.

The total length of the network $\mathcal{L} = 0.999$ m. For this length, according to the Weyl law, there should be 13 resonances in the frequency range 0.3-2.2 GHz and this is the number of resonances (fig. 15a) obtained for the network shown in figure 14c. After connecting both channels to the first vertex (fig. 14d), the number of detected resonances drops to 11. This number is consistent with the equation given in the work **(50)**, which allows to calculate the number of the resonances of the non-Weyl graph with the length $\mathcal{L}$. In this equation the length of the shortest arm connect to the balanced vertex (vertex 1) appears. In this case, this is the arm ℓ_2 at the vertex 1 and the number of the resonances for this non-Weyl network is determined by the equation:

$$N(v) = \frac{\mathcal{L}-\ell_2}{\pi} v + O(1). \qquad (10)$$

The equation was additionally verified for a pair of other networks with longer arms ℓ_1 and ℓ_2. The arms were elongated by 0.076 m. As expected, 15 resonances were obtained for Weyl network and 12 resonances for non-Weyl network (fig. 15b and d). The obtained results were confirmed by numerical calculations. The red arrows in figure 15 indicate the resonance positions obtained by means of numerical simulation.

It should be emphasised that the preparation of the vertex that makes a network a non-Weyl system turned out to be a difficult experimental challenge. A slight deviation from its symmetry caused that the graph remained a Weyl graph. The construction of such a properly operating system is therefore a significant achievement, not only from a research perspective but also from a practical point of view.

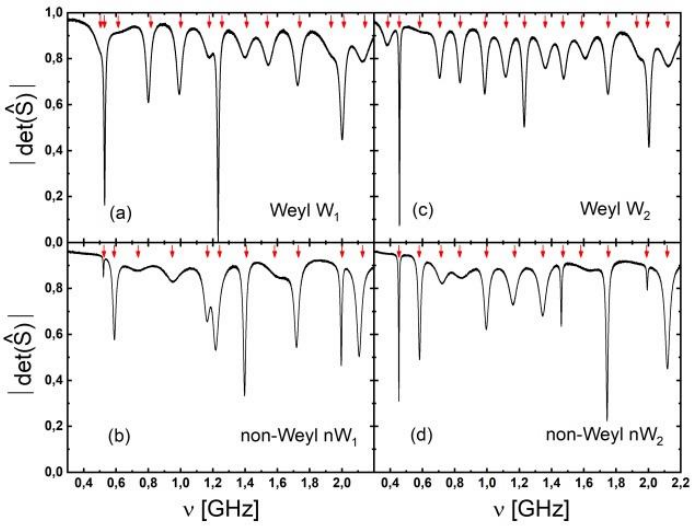

Fig. 15

Experimental spectra obtained for networks simulating Weyl and non-Weyl graphs.
a) Spectrum obtained for the channel connection ensuring a Weyl network.
b) Spectrum obtained for the channel connection ensuring a non-Weyl network.
c) Spectrum obtained for the channel connection ensuring a Weyl network after arm elongation ℓ_1 and ℓ_2.
d) Spectrum obtained for the channel ensuring a non-Weyl network after arm elongation ℓ_1 and ℓ_2.
The figure was published in H5.

Summary

The series of papers that constitutes grounds for the author's application concerning the research on the properties of chaotic microwave and quantum systems can be divided into two groups.

The first group comprising of papers **H1-H2** regarding the problem related to the analysis of spectra obtained in the experiments, i.e. the inability to detect all energy levels in the studied range and therefore, the difficulty in correctly describing the studied systems. In the paper **H1** the author presented the distributions of Wigner's reaction matrix and reflection coefficient, for microwave networks that simulate quantum graphs with broken symmetry relative to time inversion, which can be helpful in describing the systems even with strong absorption. The obtained results confirm with high accuracy the theoretical predictions. The author was the first one to experimentally verify, for GUE systems, the possibility of replacing precise formulas describing the said distributions with approximate exponential formulas. In addition, the two-port measurements were performed which allowed to detect that in the case of very high internal absorption the impact of opening channels on the system characteristics is negligible.

The paper **H2** contains a description of the procedure for verification, whether the spectrum of the studied system is a complete spectrum. For incomplete spectra, the procedure allows to determine the number of the lost energy eigenvalues. The author tested the method with GOE systems in a broad range of the number of lost states. It was verified that the proposed method is also successful for three-dimensional systems. What is particularly important, the author demonstrated that the procedure can be only used in case of random loss of eigenstates.

The second group of papers **H3-H5** concerns the research on the dependence of quantum graph properties on their topology. In the papers **H3-H4** the author presented the experimental research of two microwave networks with the same spectrum of the determinant of the four-element scattering matrix despite completely different topology. It was demonstrated that the networks have the same position of the poles of the scattering matrix and the coordinates of the poles correspond to the position and half-width of resonances. The author demonstrated the significance of ensuring appropriate boundary conditions at graph vertices. In the paper **H5** the author described an experiment in which a microwave graph that does not fulfil Weyl's law was constructed. The existence of the non-Weyl graph was confirmed to be related to the graph topology. The author demonstrated that the number of energy eigenvalues in such a graph is related to the length of a specific arm.

The microwave networks and cavities prepared and studied by the author simulate quantum graphs and billiards which are used for the studies on quantum wires, dots and other systems. The

experimental research performed by the author therefore contributed to the broadening of knowledge concerning the properties of these and other quantum systems, what is important, including but not limited, to the perspective of their future use.

References

1. H. Poincare, *Les Methodes Nouvelles de la Mechanique Celeste*, Gauthier-Villas: Paris (1892).
2. E.N. Lorenz, *Deterministic Nonperiodic Flow*, J. Atoms. Sci. **20**, 130 (1963).
3. M. L. Mehta, R*andom Matrices 2nd ed.*, Academic Press: New York (1991).
4. L. J. Pauling, Chem. Phys. **4**, 673, (1936).
5. H. Z. Jooya, K. Reihani, S.-I. Chu, Sci. Rep. **6**, 37544 (2016).
6. P. Arrighi, S. Martiel, Phys. Rev. D **96**, 024026 (2017) .
7. M. R. Brier et al.,*Neurobiology of Aging* **35**, 757 (2014).
8. M.C.Gutzwiller. *Chaos in Classical and Quantum Mechanics.* Springer-Verlag: 452, (1990).
9. T. Kottos, U. Smilansky, Phys. Rev. Lett. **79**, 4794 (1997).
10. M. Ławniczak, O. Hul, S. Bauch, P. Šeba, L. Sirko, Phys. Rev. E **77**, 056210 (2008).
11. A. Rehemanjiang, M. Allgaier, C. H. Joyner, S. Müller, M. Sieber, U. Kuhl, H.-J. Stöckmann, Phys. Rev. Lett. **117**, 064101 (2016).
12. V. Yunko, M. Białous, S. Bauch, M. Ławniczak, L. Sirko, *Experimental and numerical study of spectral properties of three-dimensional chaotic microwave cavities: The case of missing levels*, The 11th CHAOS 2018 International Conference (2018).
13. M. Białous, V. Yunko, S. Bauch, M. Ławniczak, B. Dietz, L. Sirko, Phys. Rev. E **94**, 042211 (2016). .
14. M. Ławniczak, M. Białous, V. Yunko, S. Bauch, L. Sirko, Phys. Rev. E **91**, 032925 (2015). .
15. M. Ławniczak, M. Białous, V. Yunko, S. Bauch, L. Sirko, Acta Phys. Pol. A **128**, 974 (2015).
16. M. Ławniczak, O. Hul, S. Bauch, L. Sirko, Acta Phys. Pol. A **116**, 749 (2009).
17. Y.G. Sinai, Sov. Math. Dokl. **4**, 1818 (1963).
18. F. Borgonovi, G. Casati , B. Li, Phys. Rev. Lett. **77**, 4744 (1996).
19. H. Primack, U. Smilansky, Phys. Rev. Lett. **74**, 4831 (1995).
20. A. Frisch, M. Mark, K. Aikawa, F. Ferlaino, J. Bohn, C. Makrides, A. Petrov, S. Kotochigova, Nature (London) **507**, 475 (2014).
21. J. Mur-Petit, R. A. Molina, Phys. Rev. E **92**, 042906 (2015).
22. H. I. Liou, H. S. Camarda, F. Rahn, Phys. Rev. C **5**, 131 (1972).

23. T. Zimmermann, H. Koppel, L. S. Cederbaum, G. Persch, W. Demtroder, Phys. Rev. Lett. **61**, 3 (1988).
24. D.V. Savin, H.-J. Sommers, Y. V. Fyodorov, JETP Lett. **82**, 544 (2005). .
25. Y.V. Fyodorov, D.V. Savin, H.-J. Sommers, Scattering, J. Phys. A **38**, 10731 (2005).
26. W. Kretschmer, M. Wangler, Phys. Rev. Lett. **41**, 1224 (1978).
27. J. J. M. Verbaarschot, Ann. Phys. (NY) **168**, 368 (1986).
28. Y. Kharkov, V. Sokolov, Phys. Lett. B **718**, 1562 (2013).
29. D. V. Savin, Y. V. Fyodorov, H.-J. Sommers, Acta Phys. Pol. A **109**, 53 (2006).
30. C. Fiachetti, B. Michielsen, Electron. Lett. **39**, 1713 (2003).
31. J.-H. Yeh, Z. Drikas, J. Gil Gil, S. Hong, B. T. Taddese, E. Ott, T. M. Antonsen, T. Andreadis, S. M. Anlage, Acta Phys.Pol. A **124**, 1045 (2013).
32. M. Ławniczak, S. Bauch, O. Hul, L. Sirko, Phys. Rev. E **81**, 046204 (2010).
33. H. Alt, C. Dembowski, H.D. Graf, R. Hofferbert, H. Rehfeld, A. Richter, R. Schuhmann, T. Weiland, Phys. Rev. Lett. **79**, 1026 (1997).
34. B. Eckhardt, U. Dörr, U. Kuhl, H.-J. Stöckmann, Europhys. Lett. **46**, 134 (1999).
35. O. Bohigas, M. P. Pato, Phys. Lett. B **595**, 171 (2004).
36. M. Kac, Am. Math. Mon. **73**, 1 (1966).
37. T. Sunada, Ann. Math. **121**, 169 (1985).
38. C. Gordon, D. Webb, S. Wolpert, Inventiones Mathematicae **110**, 1 (1992).
39. C. Gordon, D. Webb, S. Wolpert, Bull. Am. Math. Soc. **27**, 134 (1992).
40. S. Sridhar, A. Kudrolli, Phys. Rev. Lett. **72**, 2175 (1994).
41. B. Gutkin, U. Smilansky, J. Phys. A **34**, 6061 (2001).
42. R. Band, O. Parzanchevski, G. Ben-Shach, J. Phys. A **42**, 175202 (2009).
43. O. Parzanchevski, R. Band, J. Geomet. Anal. **20**, 439 (2010).
44. R. Band, A. Sawicki, U. Smilansky, J. Phys. A **43**, 415201 (2010).
45. R. Band, A. Sawicki, U. Smilansky, Acta Phys. Pol. A **120**, A149 (2011).
46. H. Weyl, *Über die asymptotische Verteilung der Eigenwerte*, [w:]Nachrichten der Koniglichen Gesellschaft der Wissenschaften zu Göttingen, 110–117 (1911).
47. E. B. Davies, A. Pushnitski, Analysis and PDE **4**, 729 (2011).
48. E. B. Davies, P. Exner J. Lipovský, J. Phys. A: Math. Theor. **43**, 474013 (2010).
49. P. Exner, J. Lipovský, Phys. Lett. A **375**, 805 (2011).
50. J. Lipovský, J. Phys. A: Math. Theor. **49**, 375202 (2016).

5. Presentation of other scientific and research (artistic) achievements

M. Białous, V. Yunko, S. Bauch, **M. Ławniczak**, B. Dietz, L. Sirko, 2016, *Power spectrum analysis and missing level statistics of microwave graphs with violated time reversal invariance*, Phys. Rev. Lett. **117**, 144101

The paper contains a description of the procedure for verification whether spectrum of the studied system is a complete spectrum. For the first time, this was done for a system with broken time reversal symmetry (GUE). It was the first experimental test for systems which simulate quantum graphs.

M. Białous, V. Yunko, S. Bauch, **M. Ławniczak**, B. Dietz, L. Sirko, *Long-range correlations in rectangular cavities containing point-like perturbations* Phys. Rev. E **94**, 042211 (2016).

Spectral power of discrete and finite series $S(\tilde{k})$ for rectangular microwave resonance cavity with two antennas was established in the paper. The antennas acting as scatterers caused that the system simulated a quantum billiard in the transient area between a regular and a chaotic system. The results were compared with numerical calculations, in which the antennas were accounted for as point scatterers. The comparison demonstrated compliance with the experimental results and that such a system can be treated as a semi-Poisson system.

M. Ławniczak, M. Białous, V. Yunko, S. Bauch, L. Sirko, 2015, *Experimental investigation of the elastic enhancement factor in a transient region between regular and chaotic dynamics*, Phys. Rev. E **91**, 032925

In this work, the author was the first to experimentally analyse the elastic enhancement factor for the system in the transition region between the regular and chaotic systems. He showed that this coefficient can be a good measure of the degree of chaoticity of the system. The obtained results were compared with the experimental results obtained for a chaotic system with similar absorption, as well as with the results of numerical calculations based on the random matrix theory.

M. Ławniczak, M. Białous, V. Yunko, S. Bauch, L. Sirko, *Numerical and Experimental Studies of the Elastic Enhancement Factor for 2D Open Systems*, Acta Phys. Pol. A 128, 974 (2015)

In this work, the author continued to analyse the elastic enhancement factor for the system in the transition region between the regular and chaotic systems. The obtained experimental results were compared with numerical calculations as function of the absorption not only for the regular system, where $\kappa = 0$, but also with the results of calculations for $\kappa = 2.8$, i.e. $W_{\beta=1}(\gamma, \kappa = 2.8)$ ($\kappa \to \infty$ for chaotic systems and $\kappa = 0$ for regular circuits). The comparison of results shows that the author's calculations correspond to the experimental results within the limits of experimental error, therefore indicating that the enhancement factor is a good measure of the chaoticity of a system.

M. Ławniczak, S. Bauch, O. Hul, L. Sirko, *Experimental investigation of microwave networks simulating quantum chaotic systems: the role of direct processes*, Phys. Scr. **T147**, 014018 (2012).

In this paper it was demonstrated that the distribution of the elastic enhancement factor as the function of system absorption does not depend on the so-called 'direct processes.' Such processes are related to the imperfect coupling of the experimental setup to the measured systems. The experiments were performed for microwave networks simulating quantum graphs with and without broken time reversal symmetry.

M. Ławniczak, A. Borkowska, O. Hul, S. Bauch, L. Sirko, *Experimental determination of the autocorrelation function of level velocities of microwave networks simulating quantum graphs*, Acta Phys. Pol. A **120**, 185 (2011).

In the paper the authors present the experimental distribution of the autocorrelation function of energy levels obtained for a hexagonal microwave network simulating a quantum graph with time reversal symmetry.

M. Ławniczak, Sz. Bauch, O. Hul, L. Sirko, *Experimental investigation of the enhancement factor and the cross-correlation function for graphs with and without time-reversal symmetry: the open system case*, Phys. Scr. **T143**, 014014 (2011).

The use of the cross-correlation function in distinguishing symmetry classes defined in RMT was presented in the paper. The authors demonstrated that the removal of the effect of direct processes

from the scattering matrix spectrum makes the method more effective. The distribution of the elastic enhancement factor, for microwave networks simulating graphs with and without time reversal symmetry, as the function of absorption was shown.

M. Ławniczak, S. Bauch, O. Hul, L. Sirko , *Experimental investigation of the enhancement factor for microwave irregular networks with preserved and broken time reversal symmetry in the presence of absorption*, Phys. Rev. E **81**, 046204 (2010).

In this paper, the experimental distribution of the elastic enhancement factor as the function of absorption was shown for the first time for microwave networks simulating quantum graphs with broken time reversal symmetry (GUE). Results for networks simulating GOE systems were also presented.

M. Ławniczak, O. Hul, S. Bauch, L. Sirko, *Experimental and numerical studies of one-dimensional and three-dimensional chaotic open systems*, Acta Phys. Pol. A **116**, 749 (2009).

Experimental distribution of the reflection coefficient and Wigner's reaction matrix were obtained for the first time for three-dimensional microwave resonance cavities with strong absorption. Although the theoretical predictions are for quantum systems, it was demonstrated that they are also fulfilled for classic systems.

M. Ławniczak, O. Hul, S. Bauch, P. Šeba, L. Sirko, *Experimental and numerical investigation of the reflection coefficient and the distributions of Wigner's reaction matrix for irregular graphs with absorption*, Phys. Rev. E **77**, 056210 (2008).

Experimental distribution of the reflection coefficient and Wigner's reaction matrix were obtained for the first time for chaotic systems with time reversal symmetry preserved, i.e. GOE systems. The results were obtained from single-port measurements of scattering matrix spectra.

M. Ławniczak, *Wyznaczenie temperaturowej zależności efektywnego kwadratowego współczynnika elektrooptycznego* $|n_e^3 g_{3333} - n_o^3 g_{1133}|$ *w krysztale DKDP,* (2006)

In his master thesis, the author obtained the temperature dependence of effective electro-optical square coefficient $|n_e^3 g_{3333} - n_o^3 g_{1133}|$ in a DKDP crystal that has not been studied before.

Ławniczak.